UV−Raman Characterization of Iron Peroxo Adsorbates on Fe/MFI Catalyst with High Activity for NO_x Reduction

Zhi-Xian Gao, Hack-Sung Kim, Qi Sun, Peter C. Stair,* and Wolfgang M. H. Sachtler

Center for Catalysis and Surface Science, Institute for Environmental Catalysis, and Department of Chemistry, Northwestern University, Evanston, Illinois 60208

Received: December 31, 2000; In Final Form: April 20, 2001

The interaction of O_2 with Fe supported on zeolite MFI has been investigated by the in situ UV Raman technique. Previously, the formation of adsorbed superoxide ions, O_2^-, on the Fe/MFI prepared by sublimation of $FeCl_3$ vapor onto HMFI, was identified by ESR at 77 K. In situ Raman data indicate that adsorbed peroxide ions, O_2^{2-}, are formed on the same catalysts with Fe/Al = 1 even at 300 K. A band at 730 cm^{-1}, which was found to be sensitive to the partial pressure of O_2, is tentatively assigned to the stretching vibration of peroxide ions. With the $^{18}O_2$ isotope, a red shift of 32 cm^{-1} was observed for the 730 cm^{-1} band. Raman features of other catalyst samples show that the binuclear iron sites in the Fe/MFI are essential for the formation of peroxide ions. As proposed before, the same bridging sites between two Fe ions, that are occupied by O^{2-} in the calcined catalyst, are also able to adsorb di-oxygen complexes.

1. Introduction

Certain preparations of Fe/MFI and Co/MFI are known to be active and selective catalysts for the reduction of NO_x with hydrocarbons in the presence of excess oxygen and water vapor.[1,2] The active centers in Fe/MFI are assumed to be binuclear, oxygen-bridged iron complexes, as follows from H_2-TPR, CO-TPR, and ESR data of this laboratory[1,3] and EXAFS and XANES results obtained by other research groups.[4,5] Formation of nitro groups or nitrate ions (often lumped together as "NO_y groups") on such centers is assumed to be a critical step in the catalytic reduction of NO_x. For the oxidation of NO to NO_2 or NO_3^- ions, some active forms of adsorbed oxygen have been implicated such as superoxide ions O_2^- and peroxide ions O_2^{2-}, besides the bridging oxygen of the binuclear Fe complex. Indirect evidence for an active form of adsorbed diatomic oxygen on Fe/MFI was provided by Lobree et al.[6] and Chen et al.[3] Mestl et al. identified adsorbed peroxide ions by Raman spectroscopy on La_2O_3 and defect-rich Ba/MgO[7−11] and proposed that these peroxide ions are involved in the formation of nitro intermediates and thus also in the catalytic decomposition of nitrogen oxide. They also showed that these ions are crucial intermediates in the selective oxidation of methane.[7] Recent kinetic data show the highest formation rate of NO_y on Fe/MFI, if the catalyst was first reduced, then exposed to O_2 at room temperature, followed by exposure to NO.[12] These data suggest that O_2^{2-} can replace the bridging O^{2-} ion in the binuclear iron complex. Results of CO oxidation with preadsorbed $^{18}O_2$ on such catalysts support an important role of diatomic oxygen adsorbates.

ESR data confirm the formation of O_2^- ions on Fe/MFI and Co/MFI at 77 K.[3,13] At higher temperature, the superoxide is likely to transform to a peroxo group which will be ESR silent.[14] DFT calculations by Siegbahn and Crabtree show that bridging peroxo groups are rather stable.[15] Symmetric peroxo groups cannot be detected by IR spectroscopy; such groups can, however, be identified by EELS, photoemission,[16] and Raman spectroscopy.[17,18]

In the present work, in situ UV Raman spectroscopy has been used for the detection of diatomic oxygen adsorbates on Fe/MFI catalyst. The advantages of UV Raman technique have been described elsewhere.[19,20]

For materials that are opaque in the UV, Raman spectroscopy probes only a very thin zone near the surface. The maximum depth of the zone where Raman spectroscopy can probe is the "depth of focus", determined by the optics for collecting the scattered light. The minimum depth is the "skin depth" which is determined by the absorptivity of the sample and given by $\lambda/(4\pi k)$, where λ is the laser wavelength and k is the imaginary part of the complex refractive index of the sample.[21] The depth of focus of our instrument is estimated to be $\sim 400\ \mu$m. Since there is no direct information on the k value of the Fe/MFI and H/MFI, to the best of our knowledge, we estimate the skin depth using similar solids as models.[22] At 244 nm, the skin depth of SiO (silicon monoxide, noncrystalline) is calculated to be 32.1 nm, that of Al_2O_3 (amorphous) is 22.1 nm, that of TiO_2 (rutile) is 11.4 nm, that of $Bi_{12}GeO_{20}$ is 10.5 nm, and that of FeS_2 (iron pyrite) is 9.3 nm. Therefore, the skin depths of MFI samples are probably $> \sim$10 nm, and this will be large enough to include several layers of zeolite cages that have a pore size of about 0.6 nm.

As this thin surface layer will be most intensively heated by the laser light, weakly adsorbed molecules will not be detected easily. For powdered samples this problem can be addressed by using the "fluidized bed method", described elsewhere,[20] which keeps the powder in motion so that a given grain resides only for a short time in the zone of intensive irradiation. This precaution has been used in the present work when relatively cheap gases were used, but static conditions were applied in the measurements with $^{18}O_2$.

The present research is directed toward verification of the model that adsorbed diatomic oxygen adsorbates are preferentially formed on binuclear iron complexes after removal of their bridging oxygen by a reductive treatment. To check this model,

* Corresponding author. Fax: 847-467-1018. E-mail: pstair@northwestern.edu.

10.1021/jp004619z CCC: $20.00
Published on Web 06/01/2001

UV Raman measurements have been carried out with Fe/MFI samples with different contents of the binuclear iron complex and after different treatments. Fe/MFI samples with most of the Fe contained in Fe_2O_3 clusters have also been studied, as well as a sample in which these Fe_2O_3 clusters have been redispersed by a chemical treatment.

2. Experimental Section

2.1. Catalyst Samples. H/MFI zeolite was obtained from Na/MFI, provided by UOP (Si/Al = 19 and 14, Lot # 99499506001 and 13923-60, respectively), by converting it to the NH_4 form, followed by calcination. Conventional ion exchange with a dilute ammonium nitrate solution was performed three times at ambient temperature to ensure that all Na^+ ions are replaced by NH_4^+. Catalysts were calcined by gradually increasing the temperature to 550 °C in oxygen flow.

Fe/MFI-19 (the number denotes the Si/Al ratio in this notation) was prepared by the sublimation technique described previously[1]. First, iron trichloride was sublimed to H/MFI in order to substitute H^+ by $FeCl_2^+$. Then the sample was hydrolyzed and washed with DDI water to replace chloride with hydroxide ions. Finally, the catalysts was dried and calcined in oxygen at 550 °C for 4 h. The preparation of other Fe/MFI catalysts has been described in ref 23.

Fe_2O_3/MFI was prepared by incipient wetness impregnation of H/MFI-14 with $Fe(NO_3)_3$, followed by a calcination to 550 °C for 4 h. A sample called Fe,Na/MFI was obtained by treating the corresponding Fe/MFI-14 with NaOH solution at pH = 10, followed by calcination to 550 °C. Fe,H/MFI was prepared from Fe,Na/MFI by reexchanging Na^+ with NH_4^+, followed by calcination to convert NH_4^+ ions to protons.

2.2. Sample Treatment. All samples were re-treated in situ inside the Raman cell by the following procedure: heating with a ramp of 8 °C/min in flowing gas, followed by holding at a preset temperature for 1 h before cooling down. For oxidative treatments (calcination), the flow rate of pure O_2 (99.994%) was about 100 mL/min, while the temperature was raised to 500 °C. For reductive treatments, the flow rate of pure H_2 (99.99%) was about 120 mL/min, while the temperature was raised to 450 °C with a ramp of 8 °C/min.

2.3. UV Raman Spectroscopy. The UV Raman spectrometer has been described elsewhere.[20,24] It consists of a Spex 1877 triple monochromator containing an imaging photomulitplier tube (ITT F4146) and a ratemeter (model 205A-05R from Bertan Associates, Inc.). To minimize the interferences from both thermal and photo degradation it was interfaced with the novel fludized bed apparatus operating at atmospheric pressure which has been described in detail elsewhere.[24]

The 244 nm laser excitation source for UV Raman scattering is a Lexel 95-SHG (Second Harmonic Generation) Ar^+ laser equipped with a temperature-tuned intracavity nonlinear crystal, BBO (Beta barium borate: BaB_2O_4), that frequency doubles visible radiation to mid-UV.

The Raman scattered light from the sample in the fluidized bed apparatus was collected by an $AlMgF_2$-coated ellipsoidal reflector (from Opticon) using the backscattering geometry. The ellipsoidal mirror collects the scattered light at polar angles from 39.9° to 66° and all azimuthal angles about the surface normal. The laser power delivered to the sample was about 8 mW. Each spectrum was signal-averaged for 2−4 h. The slit width used was 200 μm. The accuracy of Raman shifts is estimated to be ± 5 cm^{-1} for absolute shift and ± 2 cm^{-1} for relative shift. The spectral resolution is limited by the detector to ~ 20 cm^{-1}.

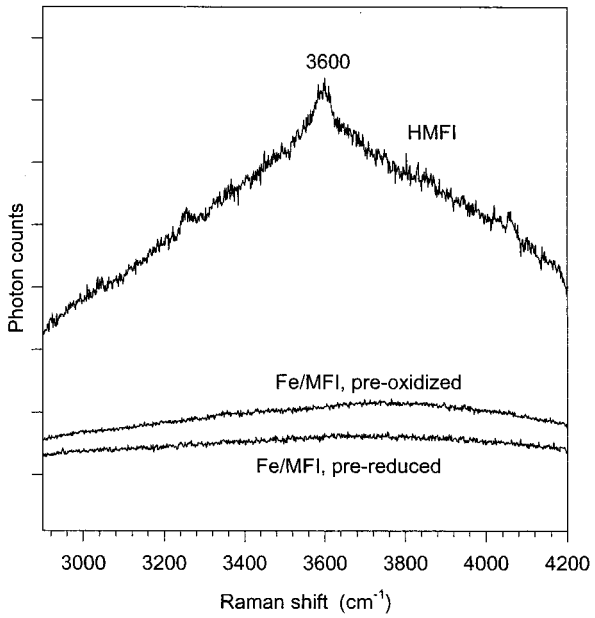

Figure 1. Raman spectra in the OH stretching region of H/MFI and Fe/MFI. All spectra were recorded in O_2 flow at room temperature.

3. Results

Figure 1 shows Raman spectra in the −OH stretching region of Fe/MFI after a variety of sample treatments. The spectrum of calcined H/MFI is also included for comparison. The Raman signal of H/MFI was more intense than that of Fe/MFI. In flowing oxygen a band at 3600 cm^{-1} was recorded on H/MFI, but no bands were observed with calcined or prereduced Fe/MFI samples. The band at 3600 cm^{-1} is assigned to the stretching of −OH groups which bridge Al and Si in the MFI type zeolite.[25] These observations are in good agreement with our previous FTIR data,[23] which confirm that the protons in the −OH group are replaced by Fe ions after sublimation of $FeCl_3$ vapor onto H/MFI.

Raman spectra of Fe/MFI in the 300∼1700 cm^{-1} region were collected in flowing O_2, He, or H_2 at room temperature with calcined and prereduced Fe/MFI. The spectra are similar in H_2 and He irrespective of the pretreatment conditions. In contrast, the spectra recorded in O_2 flow at room temperature reveal significant differences between preoxidized and prereduced Fe/MFI. These Raman spectra and the spectrum of calcined H/MFI are presented in Figure 2.

The strongest band at 380 cm^{-1} is characteristic of H/MFI. Remarkably, it is the dominant feature of H/MFI, but very weak for Fe/MFI after either treatment. With calcined Fe/MFI, several bands were recorded at 430, 490, ∼810, ∼1080, ∼1163 and 1556 cm^{-1}. The 1556 cm^{-1} band is quite sharp, with a fwhm (full width at half-maximum) of ∼20 cm^{-1}.

With the prereduced sample, an additional band at 730 cm^{-1} was observed in the presence of O_2. Interestingly, this band disappeared upon purging with He, but reappeared after exposure to O_2. This band decreased when the temperature increased in the presence of oxygen. It almost vanished at 540 K, which indicates that the chemical species associated with this band are oxygen-related and weakly adsorbed on Fe/MFI.

Figure 3 shows the Raman spectra of other related samples obtained under the same conditions. These samples were prereduced in flowing H_2 up to 400 °C, then cooled, followed by a He purge for 30 min before exposure to O_2. Only a very weak band at 730 cm^{-1} was observed over the Fe_2O_3/MFI

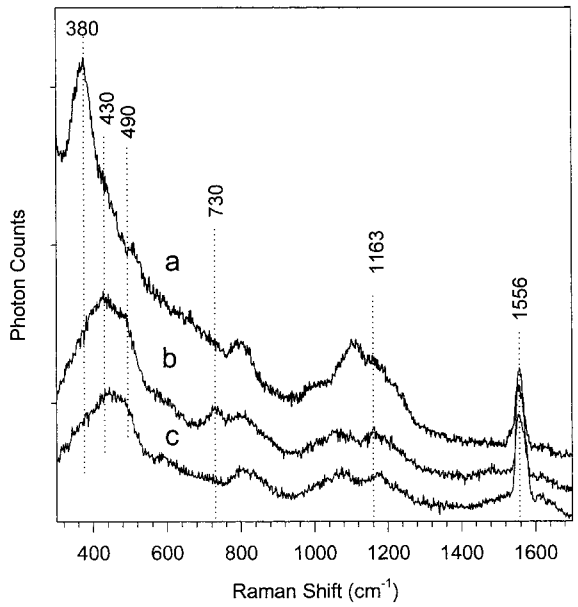

Figure 2. Raman spectra in the 300−1700 cm^{-1} region of H/MFI and Fe/MFI. All spectra were recorded in O_2 flow at room temperature: (a) preoxidized H/MFI, (b) prereduced Fe/MFI, and (c) preoxidized Fe/MFI.

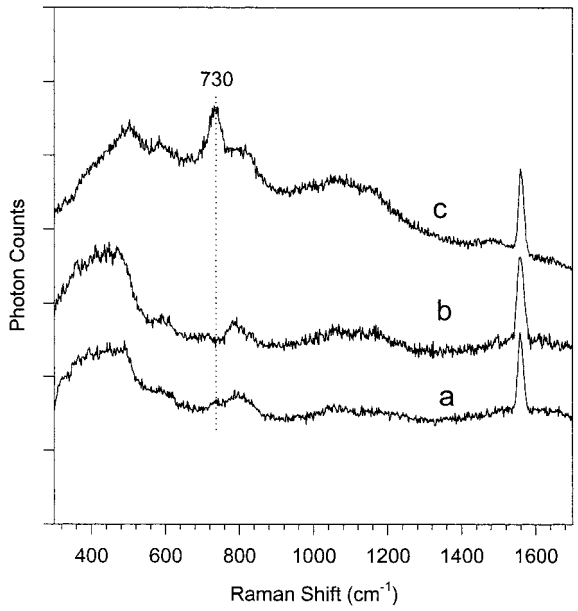

Figure 3. Raman spectra in the 300−700 cm^{-1} region of several Fe/MFI samples. All spectra were recorded in O_2 flow at room temperature after the samples were prereduced in H_2 flow: (a) Fe_2O_3/MFI, (b) Fe_2-Na/MFI, and (c) Fe,H/MFI.

sample prepared by impregnation, and the spectrum of deactivated Fe,Na/MFI did not show the band at 730 cm^{-1}. In contrast, the Raman spectrum of the reactivated Fe,H/MFI-14 sample showed a strong band at 730 cm^{-1}.

Raman spectra of the Fe,H/MFI-14 exposed to isotopomers $^{18}O_2$ and $^{16}O_2$ are depicted in Figure 4. Unlike the other spectra, those in Figure 4 were taken under static conditions and a relatively short scan time (2 h). Since the signal-to-noise ratio (S/N) is proportional to the scan time, the S/N of the spectra in Figure 4 is lower than that of the others. Furthermore, the static condition compared to the fluidized bed condition can cause more intensive heating of the probed zone by the laser, which can also contribute to the decreased intensity of the band at 730 cm^{-1} (compare Figure 3c to 4c).

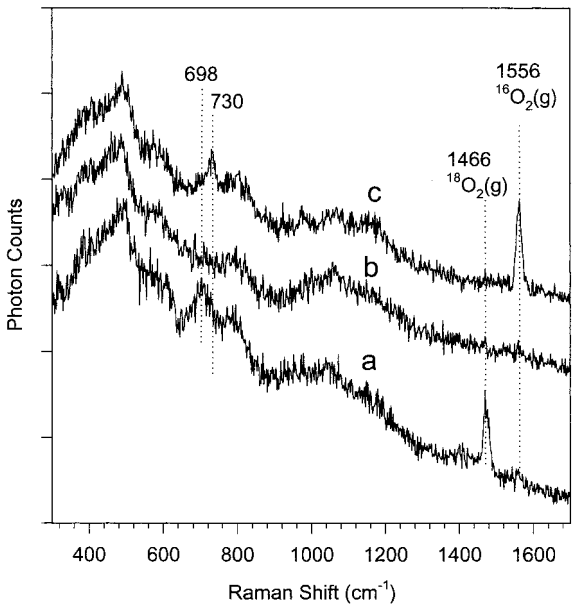

Figure 4. Raman spectra in the 300−1700 cm^{-1} region of Fe,H/MFI. All spectra were recorded at room temperature when the sample was (a) exposed to $^{18}O_2$, (b) evacuated to -10^2 Torr, and (c) exposed to $^{16}O_2$, after prereduced in H_2 flow.

The sample was first prereduced with H_2, followed by He purge for 30 min. Before oxygen gas was introduced, the Raman cell was evacuated using a mechanical pump. The background pressure in the Raman cell was subsequently lowered to $\sim 10^{-2}$ Torr. When $^{18}O_2$ was introduced in the cell, the spectrum **a** in Figure 4 was recorded. Though the partial pressure of $^{18}O_2$ was not measured, it was estimated to be ~0.75 atm based on the relative intensities of the bands due to gas oxygen in the spectra **a** and **c** in Figure 4. After evacuating the cell again to $\sim 10^{-2}$ Torr, another scan was obtained (spectrum **b**). Finally, $^{16}O_2$ at a partial pressure of 1 atm was introduced to obtain the spectrum **c** in Figure 4.

The isotopic shift is clearly demonstrated. The band at 730 cm^{-1} shifts to 698 cm^{-1} with $^{18}O_2$. The intensity of the 698 cm^{-1} band is slightly higher than that of the 730 cm^{-1} band, though the intensities of the bands for the gaseous molecules show that the $^{16}O_2$ pressure is higher than that of $^{18}O_2$. In fact the higher intensity of the 698 cm^{-1} band is mainly due to its larger width, not a greater peak height. The increased bandwidth could be due to secondary oxygen isotope exchange with the zeolite, as indicated in previous work,[26] which will produce some $^{16}O^{18}O$.

4. Discussion

4.1. Band Assignments. The band at 380 cm^{-1} (see spectrum **a** in Figure 2) is assigned to a symmetric bending vibration where the O atoms move along the bisecting line of the T−O−T angle.[27] After sublimation, the cavities of the MFI zeolite contain Fe complexes that mainly occupy the cation exchange sites, by consequence, the 380 cm^{-1} band is much weaker. Accordingly, the spectra in Figure 3 show a much stronger band at 380 cm^{-1} for Fe_2O_3/MFI and Fe,Na/MFI than for Fe,H/MFI, indicating that the iron species in Fe,H/MFI re-occupy cation sites, as was shown in ref 23. As a consequence, the other bands due to MFI zeolite should also decrease.

Bands at 430−490 cm^{-1} (see Figure 2) are also attributed to bending modes of Fe−O−O groups,[28] but these bands are very complicated and too weak to give confirmative information.

Bands in the 800−1200 cm^{-1} region (see Figure 2) were recorded on both Fe_2O_3 and H/MFI as well as MFI-supported Fe samples. The band at 800 cm^{-1} results from a Si−O and/or a symmetric T−O−T stretching vibration with a small part of oxygen movement.[27] Bands in the 960−1260 cm^{-1} region, one main peak at 1105 cm^{-1} and two shoulders at 1000 and 1170 cm^{-1}, can be attributed to T−O−T asymmetric stretching vibrations.[27]

The O−O vibration (the bond order of it is 1.5) in superoxo complexes has been observed in the 1015−1180 cm^{-1} region on various solids.[30] Since the intensity ratio of the 1163 cm^{-1} to the ∼1080 cm^{-1} band is slightly higher for oxygen on the prereduced Fe/MFI than on the preoxidized Fe/MFI (compare Figure 2b to Figure 2c and Figure 4b to Figure 4c), the 1163 cm^{-1} might contain a contribution of the superoxo species. Whether the 1163 cm^{-1} band is due to the superoxo species or to a T−O−T asymmetric stretching vibration of the zeolite lattice can be resolved in the future by careful ^{18}O labeling studies.

The sharp band centered at 1556 cm^{-1} appeared only when oxygen flows through the cell and is attributed to gaseous O_2. Since this band is not always symmetrical and has a varying bandwidth at half-maximum on all catalysts, it may result from a combination of gas-phase oxygen and physisorbed O_2 that interacts weakly with the catalyst surface.[29]

Of particular interest for the present study is the 730 cm^{-1} band that was observed at room temperature on prereduced Fe/MFI in the presence of O_2. As it is sensitive to O_2, we tentatively assign it to the O−O vibration of peroxide groups. The observed red shift from $^{16}O-^{16}O$ to $^{18}O-^{18}O$ was 32 cm^{-1} which is slightly lower than the 41 cm^{-1} calculated from the reduced mass ratio. For the gas-phase O_2 molecules a red shift of 90 cm^{-1} was observed while 89 cm^{-1} is calculated.

The bond orders of the O−O bond for the gas-phase O_2 molecules and for the free peroxide ions are calculated to be 2.0 and 1.0, respectively. Since the O−O stretching frequency for the gas-phase O_2 molecules is observed at 1556 cm^{-1}, the O−O stretching frequency for the unperturbed peroxide ions is estimated to be observed at ∼778 cm^{-1}. Actually, the O−O vibration in peroxide complexes has been observed in the 640−970 cm^{-1} region on various samples.[30] Dioxygen complexes in metal coordination compounds are well-known.[31,32] Pt and Ag metal surfaces chemisorb molecular oxygen at temperatures below 120 K. The dioxygen complex on Pt(111) [33] and Ag-(110) [34,35] have O−O stretching frequencies of 870 and 640 cm^{-1}, respectively. A frequency of 870 cm^{-1} for adsorbed dioxygen corresponds to an O−O bond order of 1.1, and that of 640 cm^{-1} corresponds to 0.8.

4.2. The Chemistry of Diatomic Oxygen Formation. To verify that the peroxo group causing the 730 cm^{-1} band is associated with binuclear iron ions, three samples were studied with identical overall composition but different content of binuclear iron ions. They are called Fe_2O_3/MFI-14, Fe,Na/MFI-14, and Fe,H/MFI-14, respectively, their Raman spectra are shown in Figure 3. Sample Fe_2O_3/MFI-14 was prepared by impregnation; it contains mainly Fe_2O_3 particles at the external surface of the zeolite. This sample is therefore a poor catalyst for selective catalytic reduction of NO_x. Indeed, the 730 cm^{-1} band is rather weak in comparison to that found with Fe/MFI. The Fe,Na/MFI-14 sample was obtained from Fe/MFI-14 by treating with NaOH solution. This treatment is known to induce agglomeration of binuclear iron complexes to nanoclusters inside the zeolite cavities. It shows a catalytic performance similar to

SCHEME 1

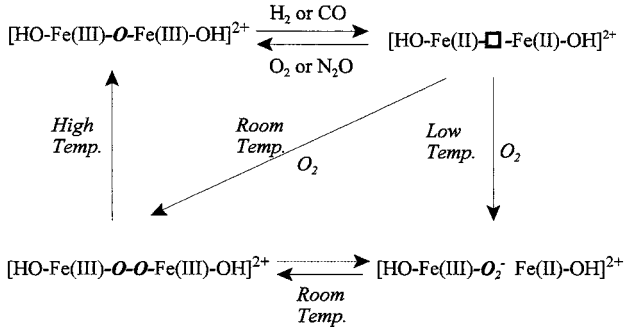

Fe_2O_3/MFI. As expected, the recorded 730 cm^{-1} band in Figure 3b is also very weak.

The third sample, Fe,H/MFI-14, was prepared by replacing the Na^+ ions in Fe,Na/MFI-14 by NH_4^+ ions, that were transformed into highly acidic H^+ ions by calcination. Previously, it has been shown that this treatment re-disperses the nanoclusters and partially regenerates the binuclear Fe oxo-ions.[23] By consequence, the catalytic activity for NO_x reduction increases. Figure 3c shows, that after reduction of this sample with H_2, followed by exposure to O_2 at room temperature, a strong Raman band appears at 730 cm^{-1}. As this band position is equal to that of the peroxo band in Fe/MFI, it confirms the model that the peroxo group is associated with the binuclear iron complex.

In addition to verifying our model, these data also provide unexpected new information. The intensity of the 730 cm^{-1} band is found to be significantly larger than that of the band in the Fe/MFI catalyst. This shows that more than simple regeneration of binuclear sites takes place. As the Fe,H/MFI-14 and the Fe/MFI samples are expected to have the same concentration of Fe, but different concentrations of protons, interaction with these Brønsted acid sites is likely responsible for the increased band intensity. It is conceivable that the effective cross section of the peroxo groups for Raman scattering is increased when acidic protons react with the binuclear iron oxo-ion, replacing one or two of its OH^- groups:

$$[HO-Fe-O-Fe-OH]^{2+} + H^+ \rightarrow [HO-Fe-O-Fe]^{3+} + H_2O$$

$$[HO-Fe-O-Fe-OH]^{2+} + 2H^+ \rightarrow [Fe-O-Fe]^{4+} + 2H_2O$$

After reduction, cooling to room temperature, and exposure to O_2, bridging peroxo groups are formed which interact electronically with Fe ions of higher effective charge than in the original complex where each Fe ion carries a hydroxyl group.

Previous work with ESR had shown that superoxide ions, with one unpaired electron, are also formed upon exposure of these catalysts to O_2 at low temperature, such as 77 K. As the present work appears to indicate formation of peroxo groups at room temperature, it is probable that these groups are more stable than superoxide ions and the latter groups are transformed into the former.[14] It follows from the DFT calculations by Crabtree et al. of systems containing di-iron configurations, that peroxide ions bridging two Fe^{3+} ions are rather stable.[15] At higher temperature, these complexes will decompose and diatomic O_2 will be either desorbed or transformed to mono-oxygen ions bridging over two iron ions. The chemistry is depicted in Scheme 1.

Acknowledgment. Financial aid from the Director of the Chemistry Division, Basic Energy Science, U.S. Department

of Energy, Grants DE-GBO2-87ER13654 and DE-FG02-97ER14789, is gratefully acknowledged. Z. X. Gao thanks the China Scholarship Council for financial support.

References and Notes

(1) Chen, H.-Y.; Sachtler, W. M. H. *Catal. Today* **1998**, *42*, 73.

(2) Wang, X.; Chen, H.-Y.; Sachtler, W. M. H. *Appl. Catal. B* **2000**, *26*, L227.

(3) Chen, H.-Y.; El-Malki, El-M.; Wang, X.; Sachtler, W. M. H. *J. Mol. Catal. A* **2000**, *162*, 159.

(4) Marturano, P.; Drozdova, L.; Kogelbauer, A.; Prins, R. *J. Catal.* **2000**, *192*, 236.

(5) Battiston, A. A.; Bitter, J. H.; Koningsberger, D. C. *Catal. Lett.* **2000**, *66*, 75.

(6) Lobree, L. J.; Hwang, I.-C.; Reimer, J. A.; Bell, A. T. *Catal. Lett.* **1999**, *63*, 233.

(7) Mestl, G.; Knözinger, H.; Lunsford, J. H. *Ber. Bunsen-Ges. Phys. Chem.* **1993**, *97*, 319.

(8) Mestl, G.; Knözinger, H. In *Handbook of Heterogeneous Catalysis*; Ertl, G., Knözinger, H., Weitkamp, J., Eds.; Wiley-Verlag Chemie: Weinheim, 1997; Vol. 2, Chapter 3.

(9) Xie, S.; Mestl, G.; Rosynek, M. P.; Lunsford, J. H. *J. Am. Chem. Soc.* **1997**, *119* (42), 10186.

(10) Mestl, G.; Rosynek, M. P.; Lunsford, J. H. *J. Phys. Chem. B* **1997**, *101*, 9321 and 9329.

(11) Mestl, G.; Rosynek, M. P.; Lunsford, J. H. *J. Phys. Chem. B* **1998**, *102*, 154.

(12) Gao, Z.-X.; Sun, Q.; Sachtler, W. M. H. *Appl. Catal.*, submitted.

(13) El-Malki, El-M.; Werst, D.; Doan, P. E.; Sachtler, W. M. H. *J. Phys. Chem. B* **2000**, *104*, 5924.

(14) Cotton, F. A.; Wilkinson, G.; Murillo, C. A.; Bochmann, M. *Advanced Inorganic Chemistry*, 6th ed.; John Wiley & Sons: New York, 1999; pp 465−471.

(15) Siegbahn, P. E. M.; Crabtree, R. H. *J. Am. Chem. Soc.* **1997**, *119*, 3103.

(16) Gland, J. L.; Sexton, B. A.; Fisher, G. B. *Surf. Sci.* **1980**, *95*, 587.

(17) Ho, R. Y. N.; Roelfes, G.; Hermant, R.; Hage, R.; Feringa, B. L.; Que, L., Jr. *Chem. Commun.* **1999**, *21*, 2161.

(18) Holland, P. L.; Cramer, C. J.; Wilkinson, E. C.; Mahapatra, S.; Rodgers, K. R.; Itoh, S.; Taki, M.; Fukuzumi, S.; Que, L., Jr.; Tolman, W. B. *J. Am. Chem. Soc.* **2000**, *122*, 792.

(19) Yu, Yi; Xiong, G.; Li, C.; Xiao, F.-S. *J. Catal.* **2000**, *194*, 487.

(20) Stair, P. C.; Li, C. *J. Vac. Sci. Technol. A* **1997**, *15* (3), 1679.

(21) Stair, P. C.; Weitz, E. *J. Opt. Soc. Am. B* **1987**, *4*, 255.

(22) Palik, E. D. *Handbook of optical constants of solids I, II, and III*; Academic Press Inc.: San Diego, 1985, 1991, and 1998.

(23) Chen, H.-Y.; Wang, X.; Sachtler, W. M. H. *Phys. Chem. Chem. Phys.* **2000**, *2*, 3083.

(24) Chua, Y. T.; Stair, P. C. *J. Catal.* **2000**, *196*, 66.

(25) Zecchina, A.; Bordiga, S.; Spoto, G.; Scarano, D.; Petrini, G.; Leofanti, G.; Padovan, M.; Arean, C. O. *J. Chem. Soc. Faraday Trans.* **1992**, *88*, 2959.

(26) Voskoboinikov, T. V.; Chen, H.-Y.; Sachtler, W. M. H. *J. Mol. Catal. A* **2000**, *155*, 155.

(27) Bauer, F.; Geidel, E.; Peuker, Ch.; Pilz, W. *Zeolites* **1996**, *17*, 278.

(28) Macdonald, I. D. G.; Sligar, S. G.; Christian, J. F.; Unno, M.; Champion, P. M. *J. Am. Chem. Soc.* **1999**, *121*, 376.

(29) Shamir, J.; Binenboym, J.; Claassen, H. H. *J. Am. Chem. Soc.* **1968**, *90*, 6223.

(30) Che, M.; Tench, A. J. *Adv. Catal.* **1983**, *32*, 1.

(31) Jones, R. D.; Summerville, D. A.; Basolo, F. *Chem. Rev.* **1979**, *79*, 139.

(32) Vaska, L. *Acc. Chem. Res.* **1976**, *9*, 175.

(33) Fisher, G. B.; Sexton, B. A.; Gland, J. L. *J. Vac. Sci. Technol.* **1980**, *17*, 144.

(34) Sexton, B. A.; Madix, R. J. *Chem. Phys. Lett.* **1980**, *76*, 294.

(35) Upton, T. H.; Stevens, P.; Madix, R. J. *J. Chem. Phys.* **1988**, *88*, 3988.